Supplementary Information

Perovskite hetero-anionic-sublattice interfaces for optoelectronics and nonconventional electronics

Dali Cheng[a], Deying Kong[b], Xing Sheng[a,c], Lan Yin[b], Huanglong Li[d*]

[a]Department of Electronic Engineering, Tsinghua University, Beijing 100084, China

[b]School of Materials Science and Engineering, Tsinghua University, Beijing 100084, China

[c]Beijing National Research Center for Information Science and Technology, Tsinghua University, Beijing 100084, China

[d]Department of Precision Instrument, Tsinghua University, Beijing 100084, China

Email: li_huanglong@mail.tsinghua.edu.cn

Figure S1

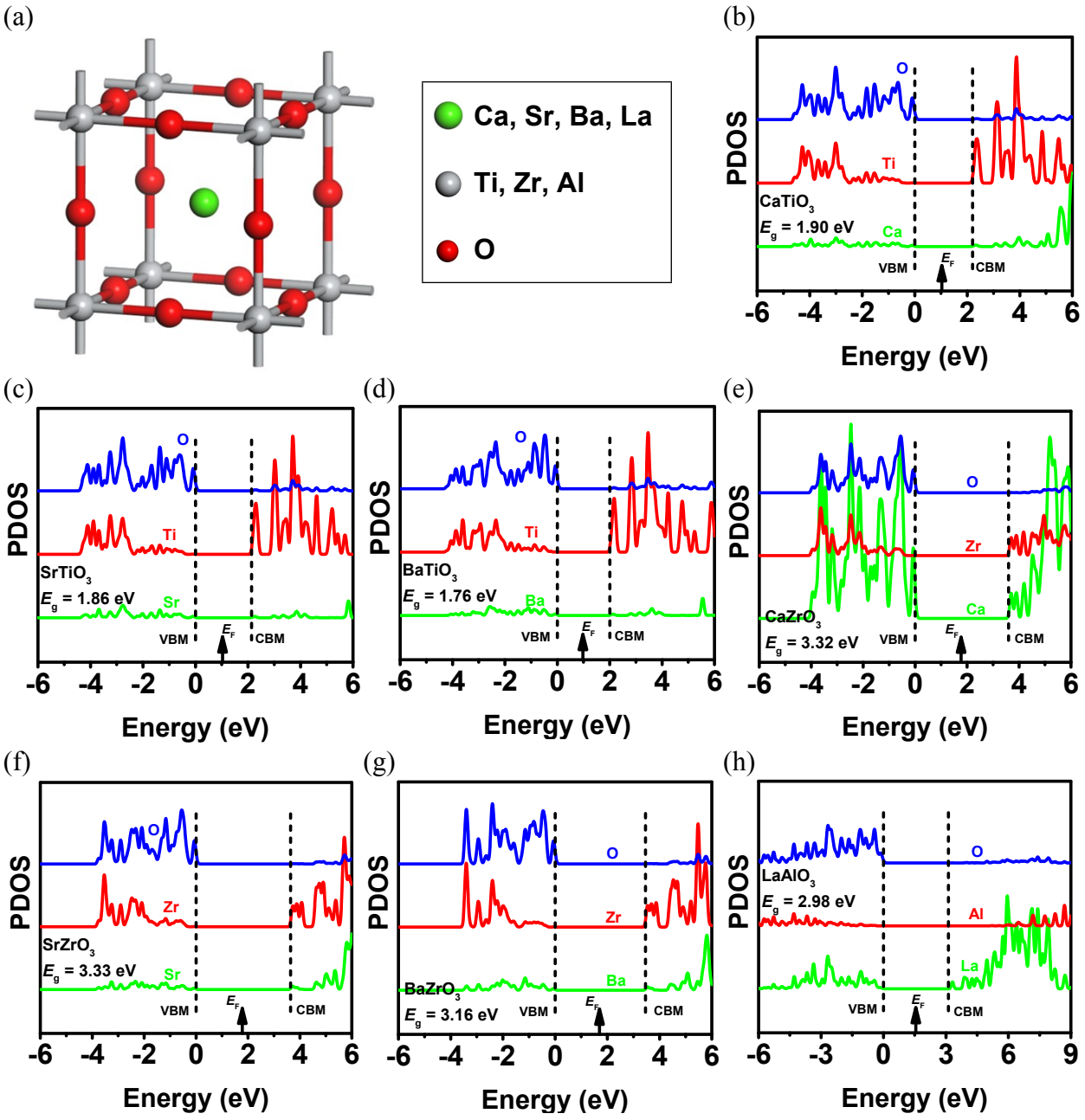

Figure S1. a) Typical atomic structure of PO. PDOSs of b) $CaTiO_3$, c) $SrTiO_3$, d) $BaTiO_3$, e) $CaZrO_3$, f) $SrZrO_3$, g) $BaZrO_3$ and h) $LaAlO_3$.

Figure S2

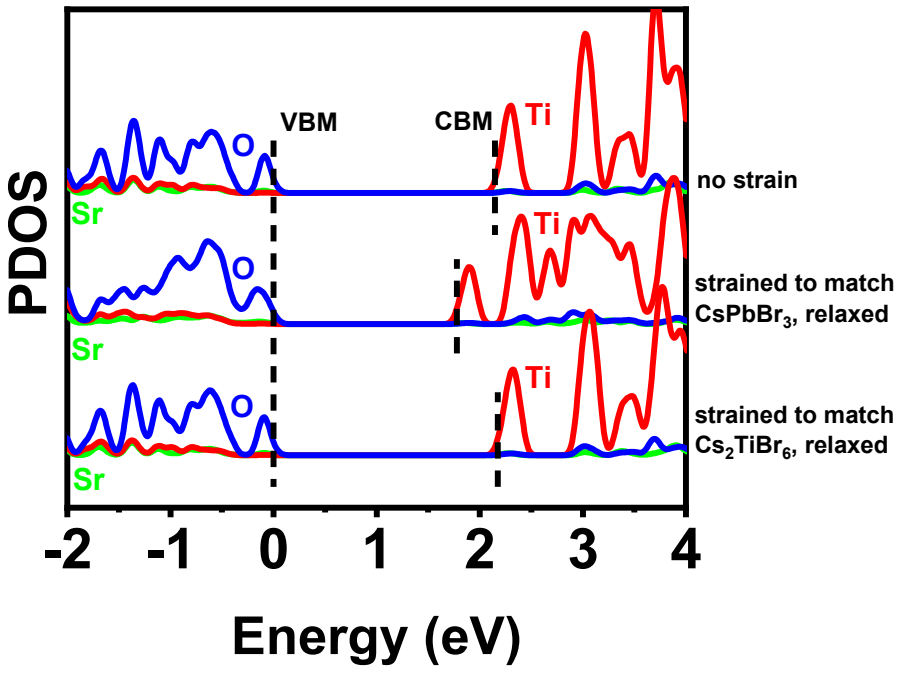

Figure S2. PDOSs of the $SrTiO_3$ unit cell under different biaxial strains.

Figure S3

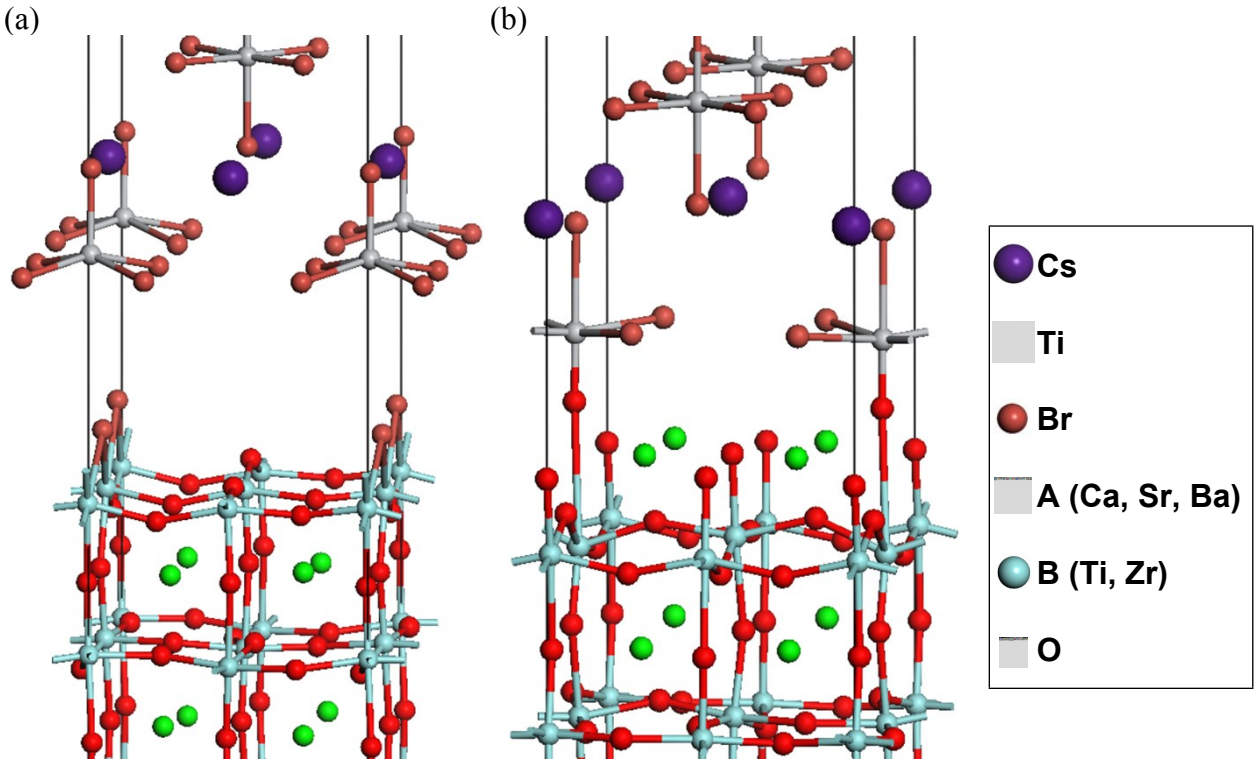

Figure S3. Atomic structures of a) type-a and b) type-b Cs_2TiBr_6: ABO_3 interfaces.

Figure S4

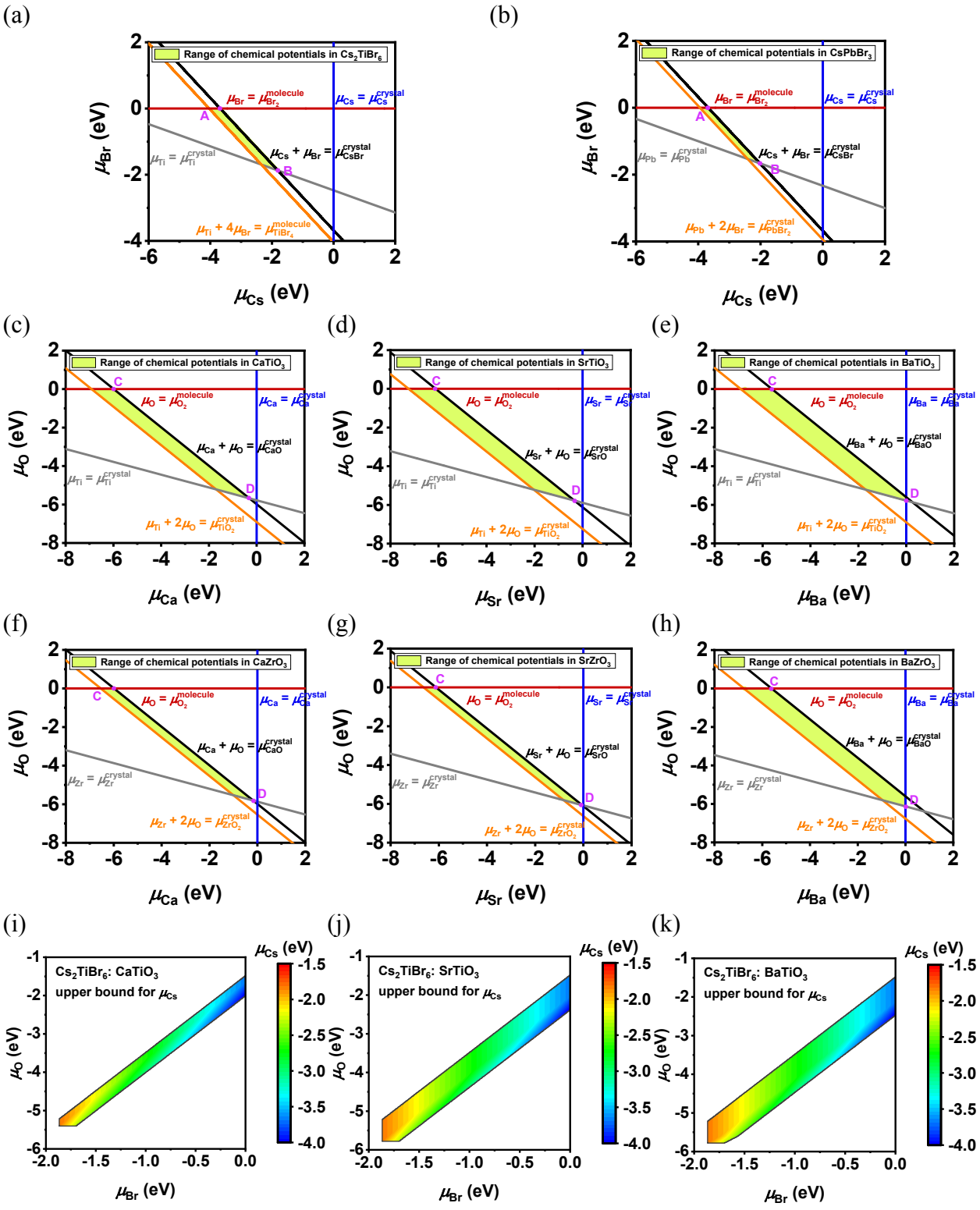
(a)
Range of chemical potentials in Cs_2TiBr_6
$\mu_{Br} = \mu_{Br_2}^{molecule}$
$\mu_{Cs} = \mu_{Cs}^{crystal}$
$\mu_{Cs} + \mu_{Br} = \mu_{CsBr}^{crystal}$
$\mu_{Ti} = \mu_{Ti}^{crystal}$
$\mu_{Ti} + 4\mu_{Br} = \mu_{TiBr_4}^{molecule}$
A
B
μ_{Br} (eV)
μ_{Cs} (eV)
(b)
Range of chemical potentials in $CsPbBr_3$
$\mu_{Br} = \mu_{Br_2}^{molecule}$
$\mu_{Cs} = \mu_{Cs}^{crystal}$
$\mu_{Cs} + \mu_{Br} = \mu_{CsBr}^{crystal}$
$\mu_{Pb} = \mu_{Pb}^{crystal}$
$\mu_{Pb} + 2\mu_{Br} = \mu_{PbBr_2}^{crystal}$
A
B
μ_{Br} (eV)
μ_{Cs} (eV)
(c)
Range of chemical potentials in $CaTiO_3$
$\mu_O = \mu_{O_2}^{molecule}$
$\mu_{Ca} = \mu_{Ca}^{crystal}$
$\mu_{Ca} + \mu_O = \mu_{CaO}^{crystal}$
$\mu_{Ti} = \mu_{Ti}^{crystal}$
$\mu_{Ti} + 2\mu_O = \mu_{TiO_2}^{crystal}$
C
D
μ_O (eV)
μ_{Ca} (eV)
(d)
Range of chemical potentials in $SrTiO_3$
$\mu_O = \mu_{O_2}^{molecule}$
$\mu_{Sr} = \mu_{Sr}^{crystal}$
$\mu_{Sr} + \mu_O = \mu_{SrO}^{crystal}$
$\mu_{Ti} = \mu_{Ti}^{crystal}$
$\mu_{Ti} + 2\mu_O = \mu_{TiO_2}^{crystal}$
C
D
μ_O (eV)
μ_{Sr} (eV)
(e)
Range of chemical potentials in $BaTiO_3$
$\mu_O = \mu_{O_2}^{molecule}$
$\mu_{Ba} = \mu_{Ba}^{crystal}$
$\mu_{Ba} + \mu_O = \mu_{BaO}^{crystal}$
$\mu_{Ti} = \mu_{Ti}^{crystal}$
$\mu_{Ti} + 2\mu_O = \mu_{TiO_2}^{crystal}$
C
D
μ_O (eV)
μ_{Ba} (eV)
(f)
Range of chemical potentials in $CaZrO_3$
$\mu_O = \mu_{O_2}^{molecule}$
$\mu_{Ca} = \mu_{Ca}^{crystal}$
$\mu_{Ca} + \mu_O = \mu_{CaO}^{crystal}$
$\mu_{Zr} = \mu_{Zr}^{crystal}$
$\mu_{Zr} + 2\mu_O = \mu_{ZrO_2}^{crystal}$
C
D
μ_O (eV)
μ_{Ca} (eV)
(g)
Range of chemical potentials in $SrZrO_3$
$\mu_O = \mu_{O_2}^{molecule}$
$\mu_{Sr} = \mu_{Sr}^{crystal}$
$\mu_{Sr} + \mu_O = \mu_{SrO}^{crystal}$
$\mu_{Zr} = \mu_{Zr}^{crystal}$
$\mu_{Zr} + 2\mu_O = \mu_{ZrO_2}^{crystal}$
C
D
μ_O (eV)
μ_{Sr} (eV)
(h)
Range of chemical potentials in $BaZrO_3$
$\mu_O = \mu_{O_2}^{molecule}$
$\mu_{Ba} = \mu_{Ba}^{crystal}$
$\mu_{Ba} + \mu_O = \mu_{BaO}^{crystal}$
$\mu_{Zr} = \mu_{Zr}^{crystal}$
$\mu_{Zr} + 2\mu_O = \mu_{ZrO_2}^{crystal}$
C
D
μ_O (eV)
μ_{Ba} (eV)
(i)
Cs_2TiBr_6: $CaTiO_3$
upper bound for μ_{Cs}
μ_{Cs} (eV)
μ_O (eV)
μ_{Br} (eV)
(j)
Cs_2TiBr_6: $SrTiO_3$
upper bound for μ_{Cs}
μ_{Cs} (eV)
μ_O (eV)
μ_{Br} (eV)
(k)
Cs_2TiBr_6: $BaTiO_3$
upper bound for μ_{Cs}
μ_{Cs} (eV)
μ_O (eV)
μ_{Br} (eV)

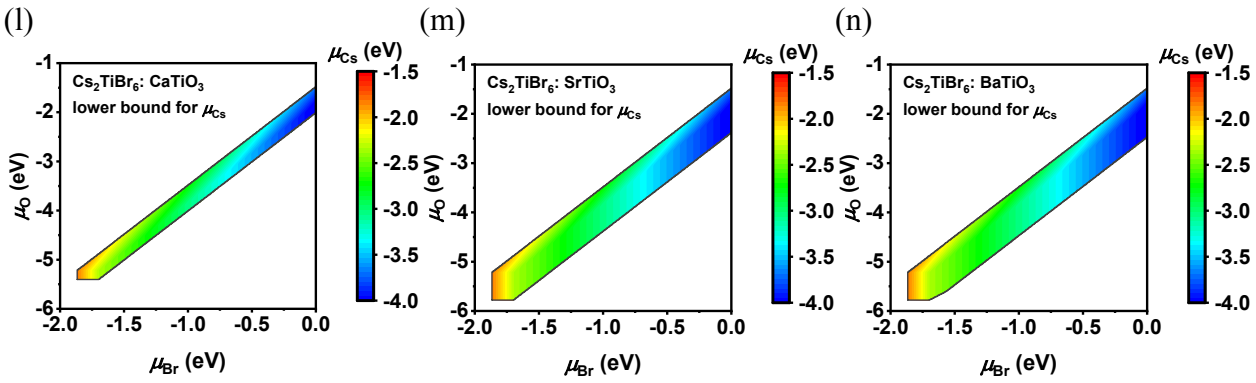

Figure S4. Ranges of atomic chemical potentials for a) Cs_2TiBr_6, b) $CsPbBr_3$, c) $CaTiO_3$, d) $SrTiO_3$, e) $BaTiO_3$, f) $CaZrO_3$, g) $SrZrO_3$ and h) $BaZrO_3$. and h) $LaAlO_3$. For Cs_2TiBr_6: $ATiO_3$ interface systems (A: Ca, Sr, Ba), the atomic chemical potentials are shown on their corresponding three-dimensional "μ_O-μ_{Br}-μ_{Cs}" color contour plots. Here, figure (i–k) and (l–n) illustrate the upper bound and lower bound values for μ_{Cs}, respectively.

Figure S5

(a)

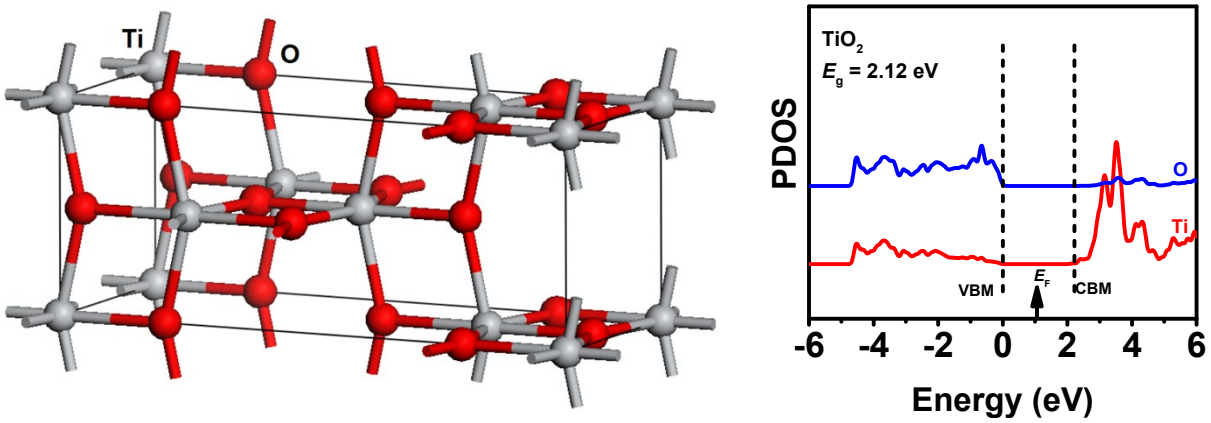

(b)

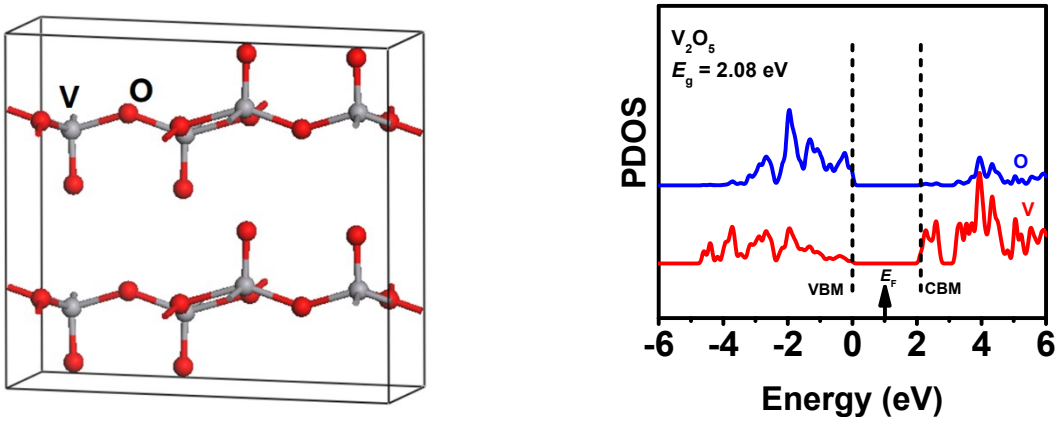

(c)

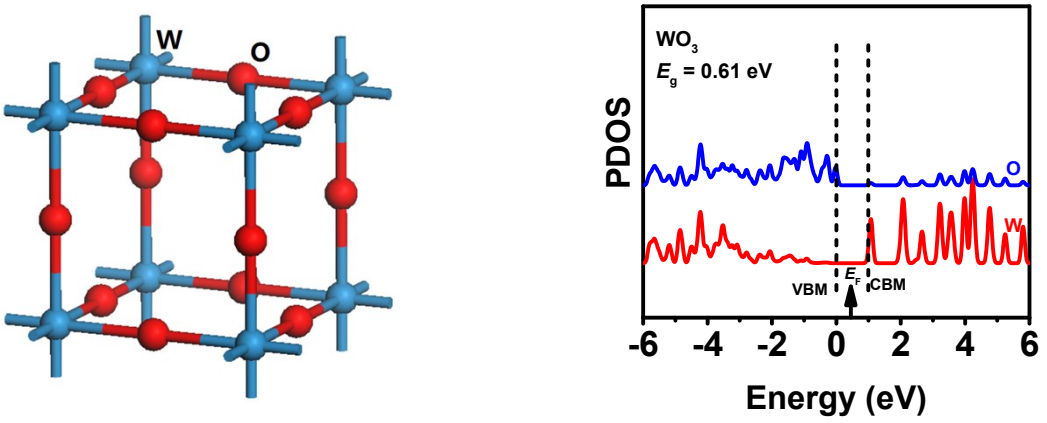

(d)

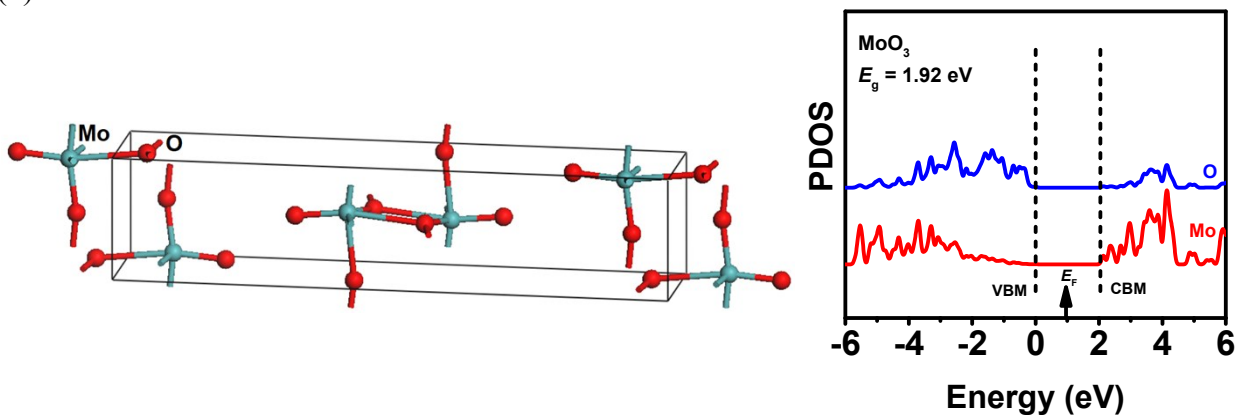

(e)

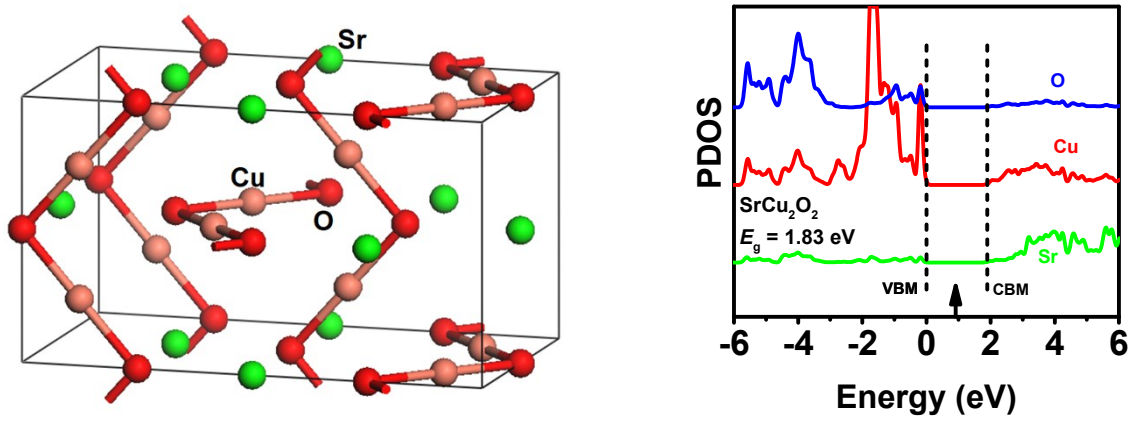

Figure S5. Atomic structures and PDOSs a) TiO_2, b) V_2O_5, c) WO_3, d) MoO_3 and e) $SrCu_2O_2$.

Figure S6

(a)

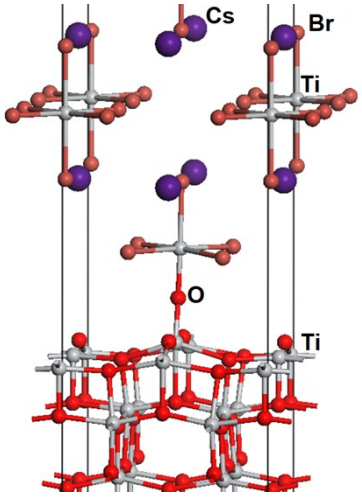

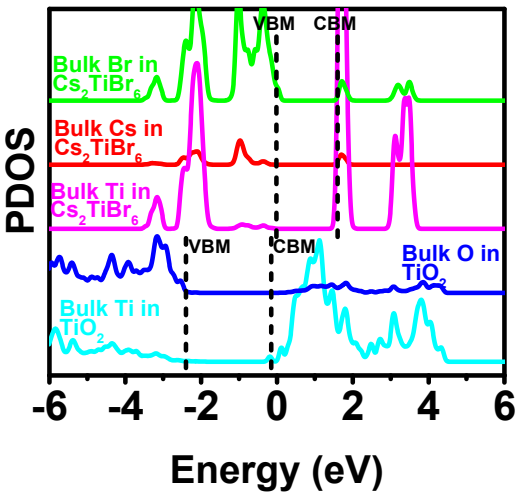

(b)

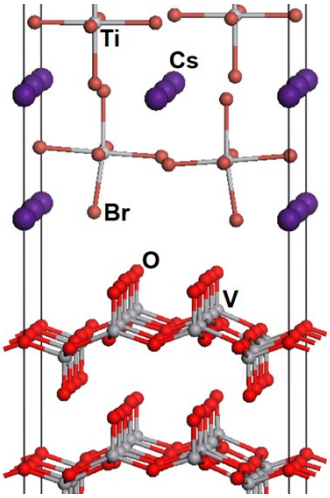

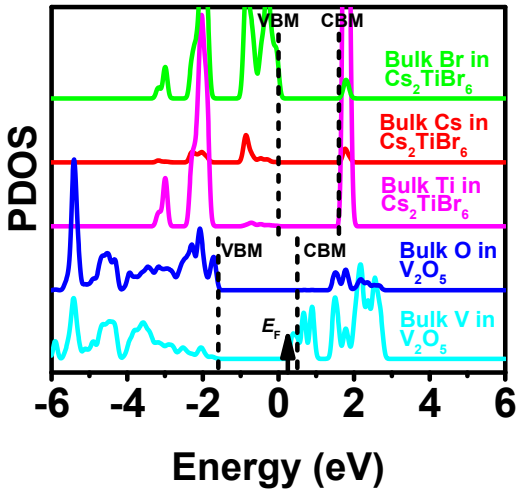

(c)

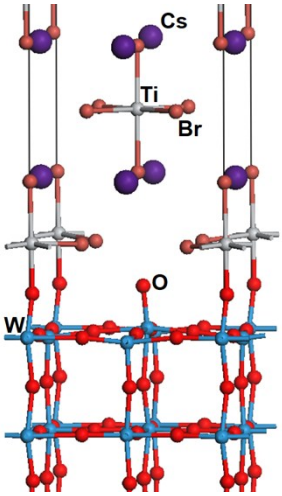

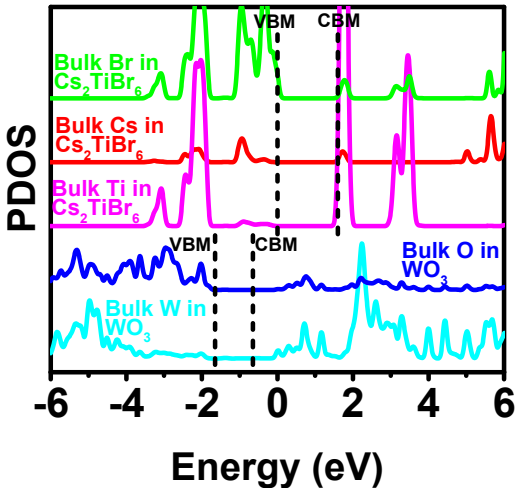

(d)

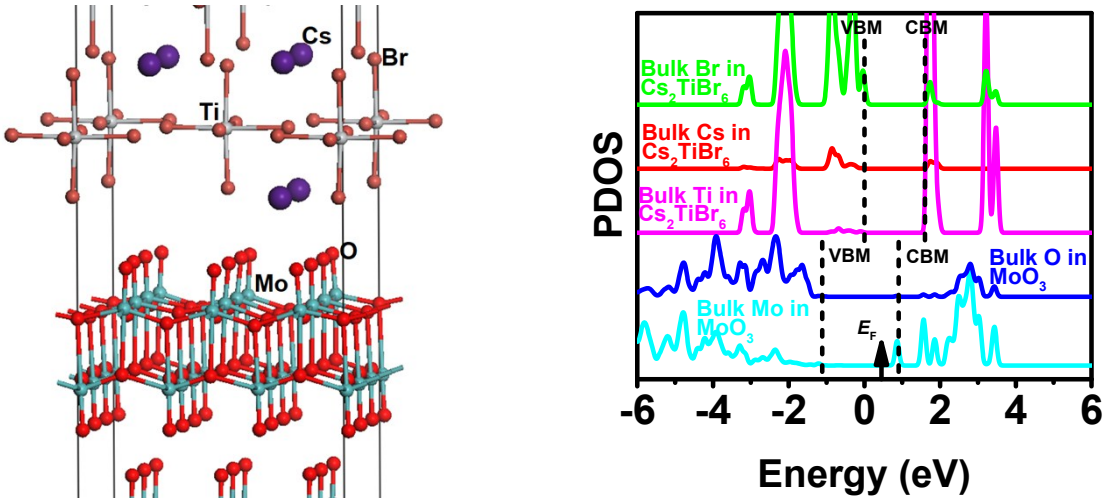

(e)

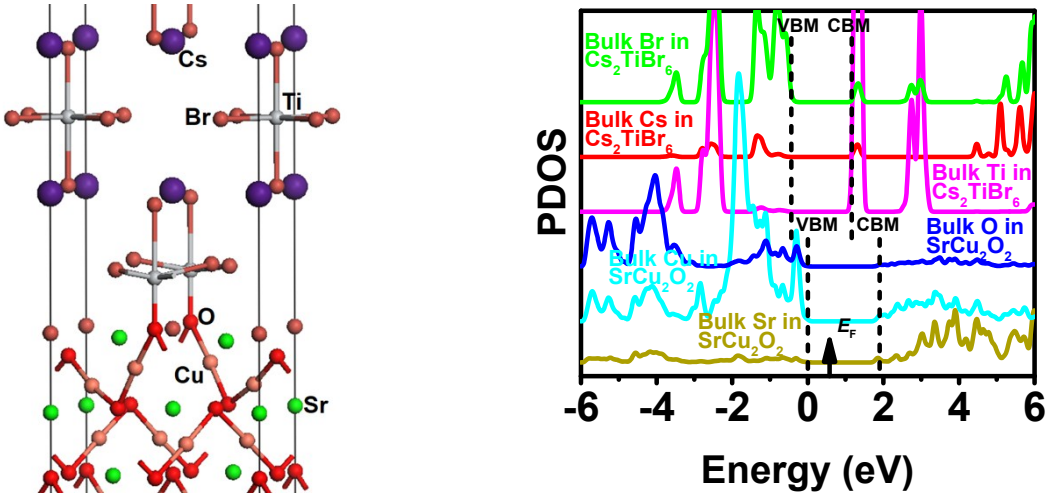

Figure S6. Atomic structures and PDOSs of a) Cs_2TiBr_6: TiO_2, b) Cs_2TiBr_6: V_2O_5, c) Cs_2TiBr_6: WO_3, d) Cs_2TiBr_6: MoO_3, and e) Cs_2TiBr_6: $SrCu_2O_2$ interfaces.

Figure S7

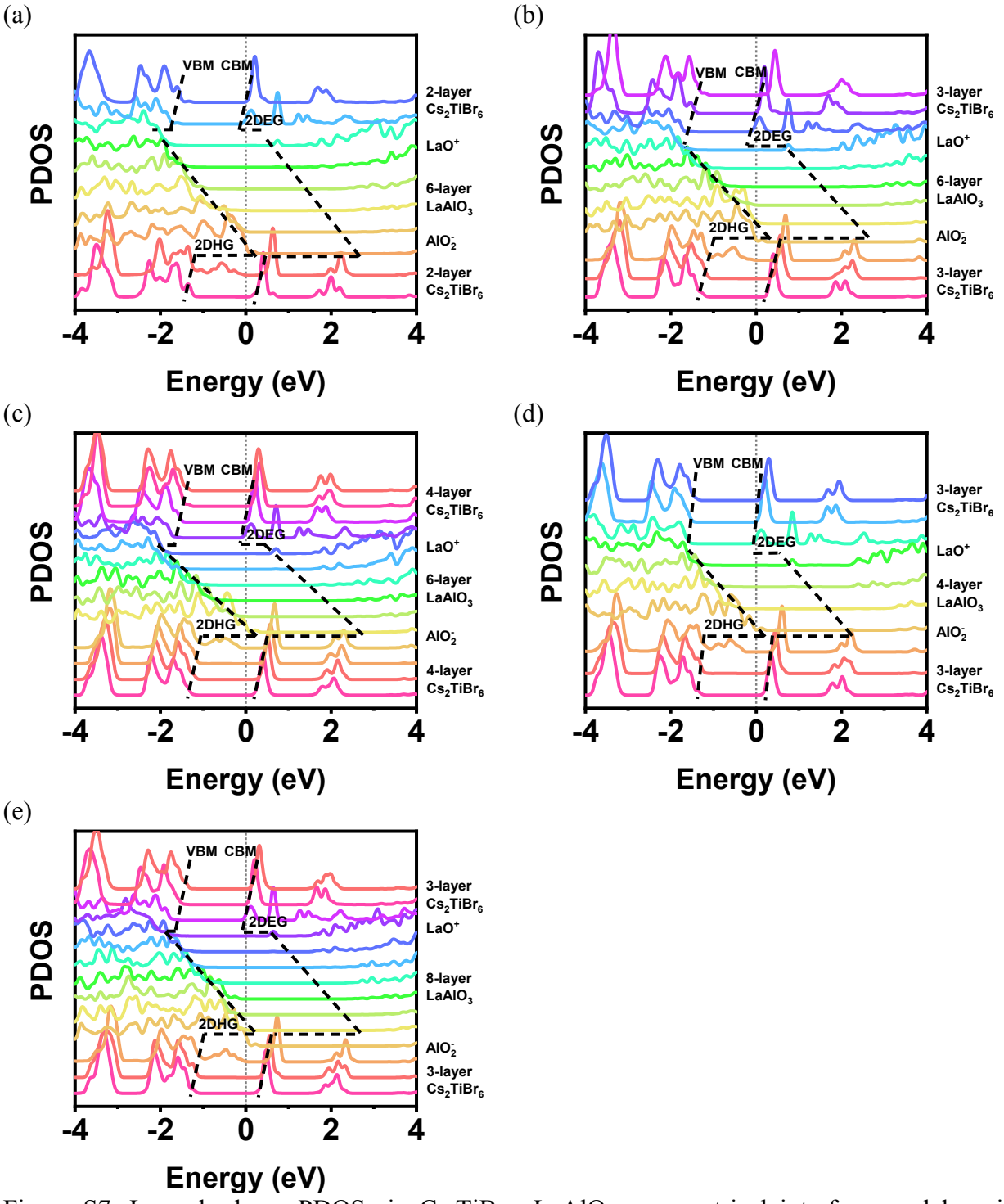

Figure S7. Layer-by-layer PDOSs in Cs_2TiBr_6: $LaAlO_3$ asymmetrical interface models, with different Cs_2TiBr_6 and $LaAlO_3$ thicknesses. a) 4-layer Cs_2TiBr_6 and 6-layer $LaAlO_3$, b) 6-layer Cs_2TiBr_6 and 6-layer $LaAlO_3$, c) 8-layer Cs_2TiBr_6 and 6-layer $LaAlO_3$, d) 6-layer Cs_2TiBr_6 and 4-layer $LaAlO_3$, and e) 6-layer Cs_2TiBr_6 and 8-layer $LaAlO_3$.

Figure S8

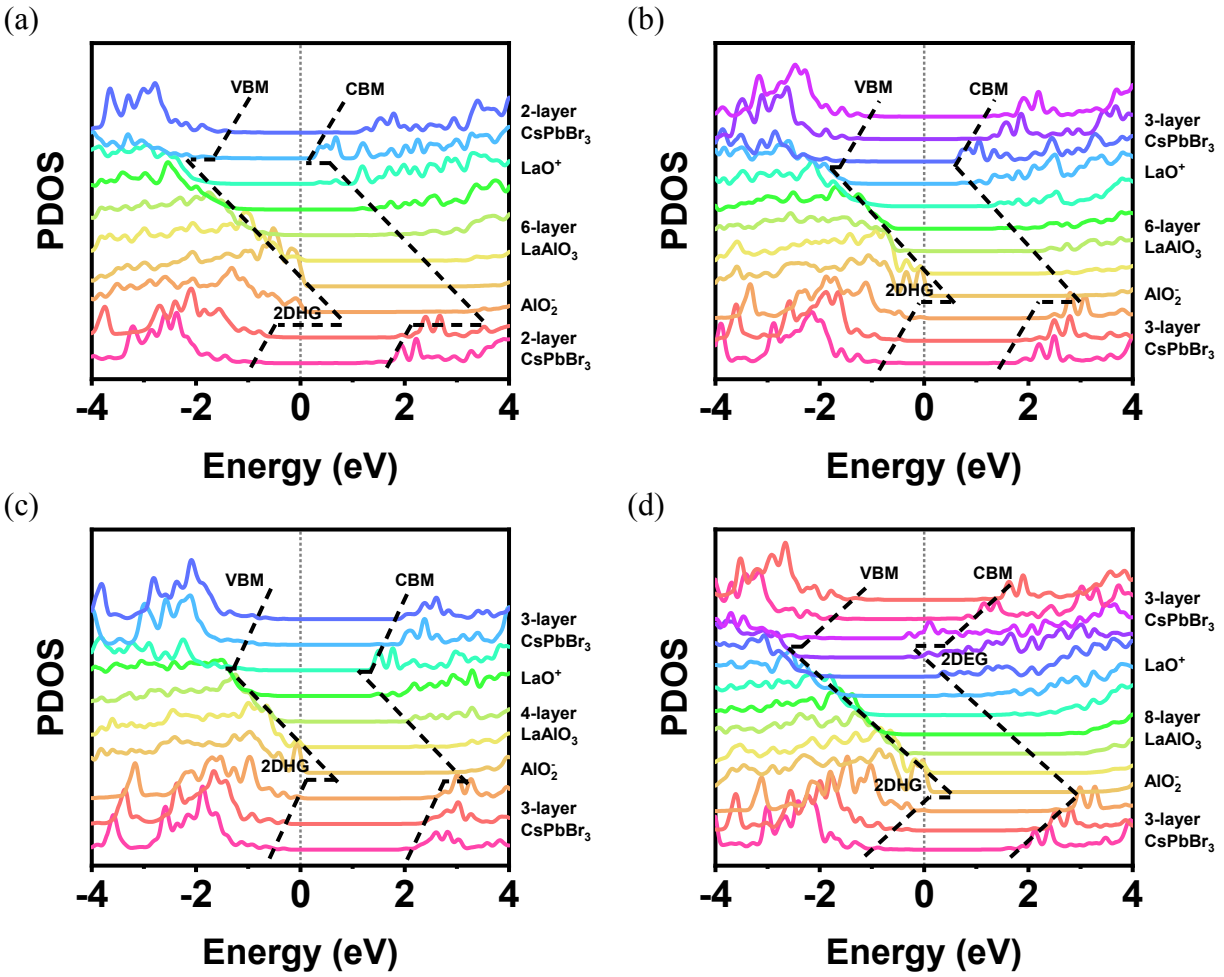

Figure S8. Layer-by-layer PDOSs in $CsPbBr_3$: $LaAlO_3$ asymmetrical interface models, with different $CsPbBr_3$ and $LaAlO_3$ thicknesses. a) 4-layer $CsPbBr_3$ and 6-layer $LaAlO_3$, b) 6-layer $CsPbBr_3$ and 6-layer $LaAlO_3$, c) 6-layer $CsPbBr_3$ and 4-layer $LaAlO_3$, and d) 6-layer $CsPbBr_3$ and 8-layer $LaAlO_3$.

Table S1

Table S1. A summary of the lattice constants of perovskite halides and perovskite oxides (unit: Å).

Material \ Lattice	a	$\sqrt{2}$ a	$2\sqrt{2}$ a
Cs_2TiBr_6	11.073	-	-
$CsPbBr_3$	6.011	-	-
$CaTiO_3$	3.885	5.494	10.988
$SrTiO_3$	3.939	5.571	11.141
$BaTiO_3$	4.026	5.694	11.387
$CaZrO_3$	4.135	5.848	11.696
$SrZrO_3$	4.171	5.899	11.797
$BaZrO_3$	4.230	5.982	11.964
$LaAlO_3$	3.838	5.428	10.856

Table S2

Table S2. Interface formation energies for $CsPbBr_3$: ABO_3 systems (unit: $eV/Å^2$). Negative value indicates that the formation of the interface is exothermic.

System	Interface Type	Chemical Potential			
		O-rich, Br-rich	O-rich, Br-poor	O-poor, Br-rich	O-poor, Br-poor
$CsPbBr_3$: $CaTiO_3$	Type a	0.1023	0.1943	-0.0548	0.0371
	Type b	-0.0335	-0.0335	-0.0335	-0.0335
$CsPbBr_3$: $SrTiO_3$	Type a	0.1356	0.2276	-0.0243	0.0677
	Type b	0.0721	0.0721	0.0721	0.0721
$CsPbBr_3$: $BaTiO_3$	Type a	0.1172	0.2092	-0.0475	0.0444
	Type b	-0.0094	-0.0094	-0.0046	-0.0046
$CsPbBr_3$: $CaZrO_3$	Type a	-0.0180	0.0740	-0.1788	-0.0868
	Type b	-0.1056	-0.1056	-0.1056	-0.1056
$CsPbBr_3$: $SrZrO_3$	Type a	0.0591	0.1510	-0.1088	-0.0168
	Type b	-0.0315	-0.0315	-0.0315	-0.0315
$CsPbBr_3$: $BaZrO_3$	Type a	0.1119	0.2039	-0.0722	0.0198
	Type b	-0.0356	-0.0356	-0.0211	-0.0211

Table S3

Table S3. Interface formation energies for Cs_2TiBr_6: $ATiO_3$ systems (unit: eV/Å^2). Negative value indicates that the formation of the interface is exothermic.

System	Interface Type	Chemical Potential			
		O-rich	O-poor	Br-rich	Br-poor
Cs_2TiBr_6: $CaTiO_3$	Type a	0.0093	0.0136	0.0099	0.0128
	Type b	-0.0063	-0.0126	-0.0109	-0.0111
Cs_2TiBr_6: $SrTiO_3$	Type a	0.0226	0.0360	0.0279	0.0291
	Type b	0.0038	-0.0147	-0.0073	-0.0049
Cs_2TiBr_6: $BaTiO_3$	Type a	0.0277	0.0412	0.0338	0.0332
	Type b	-0.0015	-0.0200	-0.0131	-0.0087

Table S4

Table S4. Interface formation energies for Cs_2TiBr_6: $AZrO_3$ systems (unit: eV/Å^2). Negative value indicates that the formation of the interface is exothermic.

System	Interface Type	Chemical Potential			
		O-rich, Br-rich	O-rich, Br-poor	O-poor, Br-rich	O-poor, Br-poor
Cs_2TiBr_6: $CaZrO_3$	Type a	-0.0031	0.0274	-0.0505	-0.0199
	Type b	-0.0498	-0.0498	-0.0498	-0.0498
Cs_2TiBr_6: $SrZrO_3$	Type a	0.0477	0.0782	-0.0018	0.0288
	Type b	0.0013	0.0013	0.0013	0.0013
Cs_2TiBr_6: $BaZrO_3$	Type a	0.0853	0.1158	0.0268	0.0573
	Type b	0.0328	0.0328	0.0413	0.0413

Table S5

Table S5. Surface energies for the component surfaces in $CsPbBr_3$: ABO_3 systems (unit: eV/Å^2). Negative value indicates that the formation of the surface is exothermic.

System	Interface Type	Component surface	Chemical Potential			
			O-rich, Br-rich	O-rich, Br-poor	O-poor, Br-rich	O-poor, Br-poor
$CsPbBr_3$: $CaTiO_3$	Type a	Halide	-0.0011	0.0908	-0.0011	0.0908
		Oxide	0.2332	0.2332	0.0760	0.0760
	Type b	Halide	-0.0188	-0.0188	-0.0188	-0.0188
		Oxide	0.0140	0.0140	0.0140	0.0140
$CsPbBr_3$: $SrTiO_3$	Type a	Halide	-0.0018	0.0902	-0.0018	0.0902
		Oxide	0.2763	0.2763	0.1164	0.1164
	Type b	Halide	-0.0207	-0.0207	-0.0207	-0.0207
		Oxide	0.0673	0.0673	0.0673	0.0673
$CsPbBr_3$: $BaTiO_3$	Type a	Halide	-0.0002	0.0917	-0.0002	0.0917
		Oxide	0.2488	0.2488	0.0840	0.0840
	Type b	Halide	-0.0190	-0.0190	-0.0190	-0.0190
		Oxide	0.0340	0.0340	0.0388	0.0388
$CsPbBr_3$: $CaZrO_3$	Type a	Halide	-0.0010	0.0910	-0.0010	0.0910
		Oxide	0.1625	0.1625	0.0018	0.0018
	Type b	Halide	-0.0199	-0.0199	-0.0199	-0.0199
		Oxide	-0.0550	-0.0550	-0.0550	-0.0550
$CsPbBr_3$: $SrZrO_3$	Type a	Halide	-0.0022	0.0898	-0.0022	0.0898
		Oxide	0.2408	0.2408	0.0730	0.0730
	Type b	Halide	-0.0198	-0.0198	-0.0198	-0.0198
		Oxide	0.0059	0.0059	0.0059	0.0059
$CsPbBr_3$: $BaZrO_3$	Type a	Halide	0.0000	0.0920	0.0000	0.0920
		Oxide	0.2814	0.2814	0.0973	0.0973
	Type b	Halide	-0.0161	-0.0161	-0.0161	-0.0161
		Oxide	0.0067	0.0067	0.0211	0.0211

Table S6

Table S6. Surface energies for the component surfaces in Cs_2TiBr_6: $ATiO_3$ systems (unit: eV/Å^2). Negative value indicates that the formation of the surface is exothermic.

System	Interface Type	Component surface	Chemical Potential			
			O-rich	O-poor	Br-rich	Br-poor
Cs_2TiBr_6: $CaTiO_3$	Type a	Halide	0.0020	0.0322	0.0010	0.0325
		Oxide	0.0430	0.0170	0.0446	0.0160
	Type b	Halide	0.0040	0.0039	0.0030	0.0040
		Oxide	0.0153	0.0093	0.0118	0.0106
Cs_2TiBr_6: $SrTiO_3$	Type a	Halide	0.0029	0.0330	0.0018	0.0334
		Oxide	0.0522	0.0354	0.0586	0.0282
	Type b	Halide	0.0041	0.0039	0.0030	0.0041
		Oxide	0.0255	0.0072	0.0155	0.0168
Cs_2TiBr_6: $BaTiO_3$	Type a	Halide	0.0033	0.0335	0.0023	0.0338
		Oxide	0.0586	0.0419	0.0657	0.0336
	Type b	Halide	0.0043	0.0041	0.0033	0.0043
		Oxide	0.0236	0.0052	0.0129	0.0164

Table S7

Table S7. Surface energies of the component surfaces in Cs_2TiBr_6: $AZrO_3$ systems (unit: eV/Å^2). Negative value indicates that the formation of the surface is exothermic.

Systems	Interface Type	Component surface	Chemical Potential			
			O-rich, Br-rich	O-rich, Br-poor	O-poor, Br-rich	O-poor, Br-poor
Cs_2TiBr_6: $CaZrO_3$	Type a	Halide	0.0036	0.0341	0.0036	0.0341
		Oxide	0.0472	0.0472	-0.0001	-0.0001
	Type b	Halide	0.0045	0.0045	0.0045	0.0045
		Oxide	-0.0397	-0.0397	-0.0397	-0.0397
Cs_2TiBr_6: $SrZrO_3$	Type a	Halide	0.0053	0.0358	0.0053	0.0358
		Oxide	0.0962	0.0962	0.0467	0.0467
	Type b	Halide	0.0057	0.0057	0.0057	0.0057
		Oxide	0.0255	0.0255	0.0255	0.0255
Cs_2TiBr_6: $BaZrO_3$	Type a	Halide	0.0059	0.0365	0.0059	0.0365
		Oxide	0.1359	0.1359	0.0774	0.0774
	Type b	Halide	0.0065	0.0065	0.0065	0.0065
		Oxide	0.0538	0.0538	0.0623	0.0623

Table S8

Table S8. Energy gains in forming the interfacial chemical bonds for $CsPbBr_3$: ABO_3 and Cs_2TiBr_6: ABO_3 systems (unit: $eV/Å^2$). Positive value indicates that the formation of the bonds is exothermic.

System	Type-a Interface	Type-b Interface
$CsPbBr_3$: $CaTiO_3$	0.1297	0.0287
$CsPbBr_3$: $SrTiO_3$	0.1388	-0.0254
$CsPbBr_3$: $BaTiO_3$	0.1313	0.0244
$CsPbBr_3$: $CaZrO_3$	0.1796	0.0307
$CsPbBr_3$: $SrZrO_3$	0.1796	0.0177
$CsPbBr_3$: $BaZrO_3$	0.1695	0.0262
Cs_2TiBr_6: $CaTiO_3$	0.0357	0.0257
Cs_2TiBr_6: $SrTiO_3$	0.0325	0.0258
Cs_2TiBr_6: $BaTiO_3$	0.0342	0.0294
Cs_2TiBr_6: $CaZrO_3$	0.0539	0.0145
Cs_2TiBr_6: $SrZrO_3$	0.0537	0.0299
Cs_2TiBr_6: $BaZrO_3$	0.0565	0.0275